Removal of Cr(VI) from aqueous solution using Fe-modified activated carbon prepared from luffa sponge: kinetic, thermodynamic, and isotherm studies

Yan-na Wang[a,1], Qun Liu[a,1], Li Shu[c], Ming-sheng Miao[a], Yu-zhen Liu[b], Qiang Kong[a,b,*]

[a]*College of Life Science, Shandong Normal University, 88 Wenhua Donglu, Jinan 250014, Shandong, P.R. China,
emails: 1461187809@qq.com (Y.-n. Wang), 373400619@qq.com (Q. Liu), mingshengmiao@163.com (M.-s. Miao),
Tel. +86 531 86182550; Fax: +86 531 86180107; email: kongqiang0531@hotmail.com (Q. Kong)*
[b]*College of Geography and Environment, Shandong Normal University, 88 Wenhua Donglu, Jinan 250014, Shandong, P.R. China,
email: 75980079@qq.com (Y.-z. Liu)*
[c]*School of Civil, Environmental and Chemical Engineering, RMIT University, Melbourne, Australia, email: li.shu846@gmail.com*

ABSTRACT

In this study, the removal of Cr(VI) from aqueous solution using Fe-modified activated carbon (AC-Fe) was investigated. AC-Fe before and after Cr(VI) adsorption was characterized by scanning electron microscopy, Fourier transform infrared spectroscopy (FTIR), and Brunauer–Emmett–Teller surface area. The effects of various parameters were investigated by batch experiments, such as contact time, temperature, pH, adsorbent dose, and initial Cr (VI). The results showed that the modification method greatly improves the adsorption property. The surface area of the activated carbon was relatively high (834.006 m^2), and the Fe-AC structure was found to be a well-developed array of microvoids and mesopores. FTIR revealed that the abundance of O–H, N–H, C–O, metal-oxygen, and metal-hydroxyl functional groups on the surface of the Fe-AC may play an important role for the adsorption of Cr(VI). The optimum pH was 1 with maximum removal efficiency of 98.71%. The batch equilibrium data fitted well to the Langmuir isotherm ($R^2 = 0.9960$) at 308 K, which indicated monolayer adsorption. Kinetic data were best fitted with the pseudo-second-order kinetic model, which was considered as the rate-limiting factor. The negative ΔG values confirmed the spontaneity of the adsorption process. Positive ΔH and ΔS values indicated endothermic and irreversible adsorption.

Keywords: Luffa sponge; Fe-modified activated carbon; Cr(VI); Adsorption

---

*Corresponding author.

[1]These authors equally contributed to this work.

1. Introduction

Chromium is defined as a poisonous heavy metal by the US Environmental Protection Agency, and trivalent chromium (Cr(III)) and hexavalent chromium (Cr(VI)) are the main oxidation states. Cr(III) is an essential trace element in the human body, especially in maintenance of glucose metabolism. Cr(VI), which is primarily present in the form of chromate (CrO_4^-) and dichromate ($Cr_2O_7^-$), possesses significantly higher levels of toxicity than the other valency states [1]. Public concern over chromium is mostly related to Cr(VI), because of its toxic, carcinogenic, and mutagenic in the nature environment and biological organism [2]. In addition, it has high water solubility and mobility over almost the entire pH range [3]. The accumulation of heavy metal ions in living tissues throughout the food chain poses a serious health problem [4]. With rapid industrialization, an increasing number of industries release polluted water containing Cr(VI) and other contaminants [5], including electroplating, leather tanning, textile, paint, and pigment industries.

There are several ways to remove heavy metal ions from aqueous solution, such as reverse osmosis [6], ion exchange [7], photocatalytic oxidation [8,9], and adsorption. Some methods have problems that limit their application, such as high energy consumption, low efficiency, high cost, and production of a large amount of wastewater. Among the many approaches to treat effluent, adsorption is the conventional method but it is not cost-effective [10–14].

Activated carbon (AC) has been used for Cr(VI) adsorption because of its large specific surface area and large number of surface active adsorption sites [15,16]. Several raw materials have been used to remove Cr(VI) from wastewater, such as *Trapa natans* husk [17] and groundnut shells [18]. To increase the adsorption capacity for metal ions, many studies have modified AC by physical or chemical treatments.

In our previous study, AC prepared from luffa sponge was used as an adsorbent to remove Cr(VI) from aqueous solution. The results indicated that its adsorption capacity is higher than other ACs produced from low-cost materials. To improve the removal performance, a number of modification methods were investigated, and modification by iron loading was the best. In this study, the adsorption isotherm, adsorption kinetics, and thermodynamics for adsorption of Cr(VI) on Fe-loaded AC (AC-Fe) were investigated. In addition, the surface area, surface structure, pore size distribution, and Fourier transform infrared (FTIR) spectrum of AC-Fe were determined. Various parameters affecting adsorption of Cr(VI) on AC-Fe were investigated, such as temperature, initial (Cr(VI)), amount of AC-Fe, and solution pH.

2. Materials and methods

2.1. Materials and chemicals

Deionized water was used to prepare all of the solutions. Luffa sponge was obtained from Jinan (Shandong, China). The pH was adjusted by adding 0.1 mol/L H_2PO_3 and NaOH. A stock solution of 1,000 mg/L Cr(VI) was prepared by dissolving 2.829 g $K_2Cr_2O_7$ (dried for 12 h in a drying oven at 100°C) in 1,000 mL deionized water. All of the different concentration solutions were prepared by appropriately diluting the stock solution. All of the chemicals used in the experiments were of analytical grade.

2.2. Preparation of AC and AC-Fe

The luffa sponge sample was rinsed, and the seeds were removed. The luffa sponge was then heated in a resistance box at 100°C for 12 h as the advanced oxidation process. The dried luffa sponge was crushed to about 2 mm in length using a high-speed grinder (HCP-100, Jinsui Company, Zhejiang, China). The crushed luffa was mixed with 0.01 mol/L $FeCl_3$ solution for 10 h at 80°C and then filtered with filter paper and dried in the resistance box for 12 h at 100°C. The above process without the modification step (mixing with $FeCl_3$ solution) was used to prepare AC. The preparation procedure for luffa sponge AC activation by H_3PO_4 was the same as our previous study [19]. The processed luffa sponge was activated by steeping it in H_3PO_4 (1 + 1) for 12 h. The solid–liquid ratio was 1:4–6 (g:mL), and the concentration of phosphoric acid was 85%. The sample was carbonized at 450°C for 1 h in a resistance box, eluted with deionized water until the pH was nearly 7, and then dried in a resistance box for 12 h at 120°C to give AC-Fe. A mortar was used to grind AC-Fe to a particle size of 150–200 mesh.

2.3. Characterization of AC-Fe and Fourier transform infrared analysis

The surface of AC-Fe was observed by scanning electron microscopy (SEM, SUPRA 55, Zeiss Company, Germany). The structural characteristics of AC-Fe and AC samples were investigated. The Brunauer–Emmett–Teller (BET) specific surface areas of the AC-Fe and AC samples were calculated using a surface area analyzer (Quantachrome, USA). A porosity

analyzer (Quadrasorb SI, Quantachrome) was used to determine the pore size distribution and porosity. Fourier transform infrared (Thermo Scientific, USA) spectra of AC-Fe before and after the adsorption experiments were recorded in the range 400–4,000 cm^{-1} using a FTIR spectrometer (Thermo Scientific, USA).

2.4. Batch adsorption experiments

To determine the optimum conditions for removal of Cr(VI) from aqueous solution, batch adsorption experiments were carried out by an oven-controlled crystal oscillator (HZQ-2, Jintan, Beijing, China) using 150-mL conical flakes with the same conditions (stirring rate 180 rpm, 50 mL solution). The effects of contact time (0–360 min), temperature (288–308 K), initial (Cr(VI)) (1–40 mg/L), AC-Fe dose (0.1–0.8 g/L), and initial pH (1–13) on adsorption were investigated. Using standard solution, the absorbance was determined using an UV–vis spectrophotometer (T6-Xinshiji, Beijing, China), and a standard curve was constructed. After equilibration and standing for 10 min, the concentration of Cr(VI) was determined using the standard curve. The adsorption amount Q_e (mg/g) and removal efficiency of Cr(VI) at equilibrium were calculated as follows:

$$Q_e = (C_0 - C_e)V/W \qquad (1)$$

$$Removal \ efficiency = 100(C_0 - C_e)/C_0 \qquad (2)$$

where C_e is the equilibrium Cr(VI) concentration (mg/L), Q_0 is the initial (Cr(VI)) (mg/L), V is the solution volume (L), and W is the mass of adsorbent (g).

2.4.1. Effect of contact time

Cr(VI) solutions with concentrations of 10, 20, and 50 mg/L were prepared using deionized water. Aliquots of the prepared solutions (50 mL) were placed in 150 mL conical flasks, and AC-Fe was added to give (AC-Fe) = 0.4 g/L. The samples were oscillated in a thermostatic oscillator, and the Cr(VI) concentration was determined at 10, 30, 60, 90, 120, 180, 240, 300, and 360 min. The equilibrium concentration and removal efficiency of Cr(VI) were determined.

2.4.2. Effect of temperature

A 20 mg/L Cr(VI) solution was used to investigate the effect of temperature. Aliquots of the Cr(VI) solution (50 mL) were added to 150 mL conical flasks, and AC-Fe was added to give (AC-Fe) = 0.4 g/L. The samples were oscillated for 240 min in the thermostatic oscillator (180 rpm), and the temperature was controlled at 288, 293, 298, 303, or 308 K. The removal efficiency of Cr(VI) and Q_e was calculated.

2.4.3. Effect of initial (Cr(VI))

Cr(VI) solutions with different concentrations were used to investigate the effect of initial (Cr(VI)). Cr(VI) solutions with concentrations from 1 to 40 mg/L were prepared with deionized water. Aliquots of the prepared solutions (50 mL) were placed in 150 mL conical flask, and AC-Fe was added to give (AC-Fe) = 0.4 g/L. The samples were oscillated for 240 min in a thermostatic oscillator (180 rpm), and the temperature was controlled at 298 K. The removal efficiency of Cr(VI) and Q_e was calculated.

2.4.4. Effect of AC-Fe dose

A 20 mg/L Cr(VI) solution was used to investigate the effect of AC-Fe dose. Aliquots of the Cr(VI) solution (50 mL) were placed in 150 mL conical flasks, and AC-Fe was added to give (AC-Fe) = 0.1–0.9 g/L. The samples were oscillated for 240 min in a thermostatic oscillator (180 rpm), and the temperature was controlled at 298 K. The removal efficiency of Cr(VI) and Q_e was calculated.

2.4.5. Effect of initial pH

A 20 mg/L Cr(VI) solution was used to investigate the effect of initial pH. Aliquots of the Cr(VI) solution (50 mL) were added to 150 mL conical flask, the pH was adjusted from 1 to 13, and AC-Fe was added to give (AC-Fe) = 0.4 g/L. The samples were oscillated for 240 min in a thermostatic oscillator (180 rpm), and the temperature was controlled at 298 K. The removal efficiency of Cr(VI) and Q_e was calculated.

2.5. Adsorption isotherm

The adsorption isotherm is crucial to optimize the use of the adsorbent, because it can be used to evaluate the adsorption capacity of the adsorbent and describe the interaction between the adsorbent and the adsorbate [20]. The process of adsorption can be divided into two types depending on the interaction between the adsorbent and the adsorbate: physical and chemical adsorption. Physical adsorption is adsorption by

weak van der Waals forces, and chemical adsorption is adsorption by chemical bonding [21].

　　Cr(VI) solutions with concentrations from 1 to 40 mg/L were prepared with deionized water, and AC-Fe was added to give (AC-Fe) = 0.4 g/L. The samples were oscillated for 240 min in a thermostatic oscillator (180 rpm), and the temperature was controlled at 288, 298, or 308 K. The linear forms of the Langmuir (Eq. (3)), Freundlich (Eq. (4)), and Dubinin–Radushkevich (Eqs. (5)–(7)) adsorption isotherms can be expressed as follows:

$$\frac{C_e}{Q_e} = \frac{1}{Q_m K_L} + \frac{1}{Q_m} C_e \tag{3}$$

$$\ln Q_e = \ln K_F + \frac{1}{n} \ln C_e \tag{4}$$

$$\ln Q_e = \ln Q_m - \beta \varepsilon^2 \tag{5}$$

$$\varepsilon = RT \ln(1 + 1/C_e) \tag{6}$$

$$E = (2\beta)^{-1/2} \tag{7}$$

In Eq. (3), Q_m is the maximum adsorption capacity (mg/g) and K_L is the Langmuir constant (L/mg), which reflects the adsorption rate. In Eq. (4), K_F is the Freundlich constant (mg/g) and n is the adsorption intensity. $1/n$ represents the adsorption capacity, where the smaller the $1/n$ value, the higher the adsorption performance. In Eq. (5), β is a constant related to the adsorption energy (kJ^2/mol^2), R is the ideal gas constant (8.314 J/(mol K)), T is thermodynamic temperature (K), and ε is the Polanyi potential. E is the average free energy of adsorption (kJ/mol).

2.6. Adsorption kinetics

　　Kinetic models can be used to investigate the rate-controlling step of adsorption and the adsorption mechanism. Three kinetic models were considered: the pseudo-first-order, pseudo-second-order, and intraparticle diffusion models.

　　The linear forms of the pseudo-first-order (Eq. (8)), pseudo-second-order [22] (Eq. (9)), and intraparticle diffusion models (Eq. (10)) can be expressed as:

$$\ln(Q_e - Q_t) = \ln Q_e - k_1 t \tag{8}$$

$$t/Q_t = 1/k_2 Q_e^2 + t/Q_e \tag{9}$$

$$Q_t = k_p t^{1/2} + C \tag{10}$$

where Q_t (mg/g) is the amount of adsorbate adsorbed at time t (min) and k_1 (1/min) is the rate constant of the pseudo-first-order model. k_2 is the rate constant of the pseudo-second-order model (g/(mg min)). k_p is the intraparticle diffusion rate constant (mg/(g min$^{1/2}$)), and C is the intercept of the plot of Q_t against t (mg/g).

2.7. Thermodynamics

　　The free energy change (ΔG), enthalpy change (ΔH), and entropy change (ΔS) of chromate reduction are related to the Langmuir coefficient (K_L) by

$$\ln K_L = \Delta S/R - \Delta H/RT \tag{11}$$

where T is the thermodynamic temperature (K). The Gibbs free energy of adsorption can be calculated by [23]:

$$\Delta G = -RT \ln K_L \tag{12}$$

3. Results and discussion

3.1. Characteristics of AC-Fe and FTIR analysis

　　The inhomogeneous pore structure of AC is important for adsorption, and many characterization methods can be used to characterize the pore structure and properties [24]. SEM, the BET surface area, and the pore size distribution were used to investigate the characteristics of AC-Fe and AC. SEM is a common way of examining the surface features of AC, and the SEM images of AC-Fe and Cr(VI)-adsorbed AC-Fe are shown in Fig. 1. The surface of AC-Fe is more rough and features a higher porpous structure than AC-Fe, which greatly raised the adsorption ability. The BET surface area of AC-Fe is 834.006 m^2/g. While, the BET surface area of AC from co-mingled waste is 638 m^2/g, the commercial norit carbon post-oxidized with 1 M HNO$_3$ is 837 mg/g, which has a high surface area as the AC-Fe [25]. Therefore, the AC-Fe may have outstanding adsorption property. The pore size distributions of AC-Fe and AC are shown in Fig. 2. From Fig. 2, it can be seen that there are abundant and inhomogeneous pores in AC-Fe and AC. It could be deduced that AC-Fe had a well-developed porous structure, which contains more microvoids with minor mesopores than AC, and the modification method
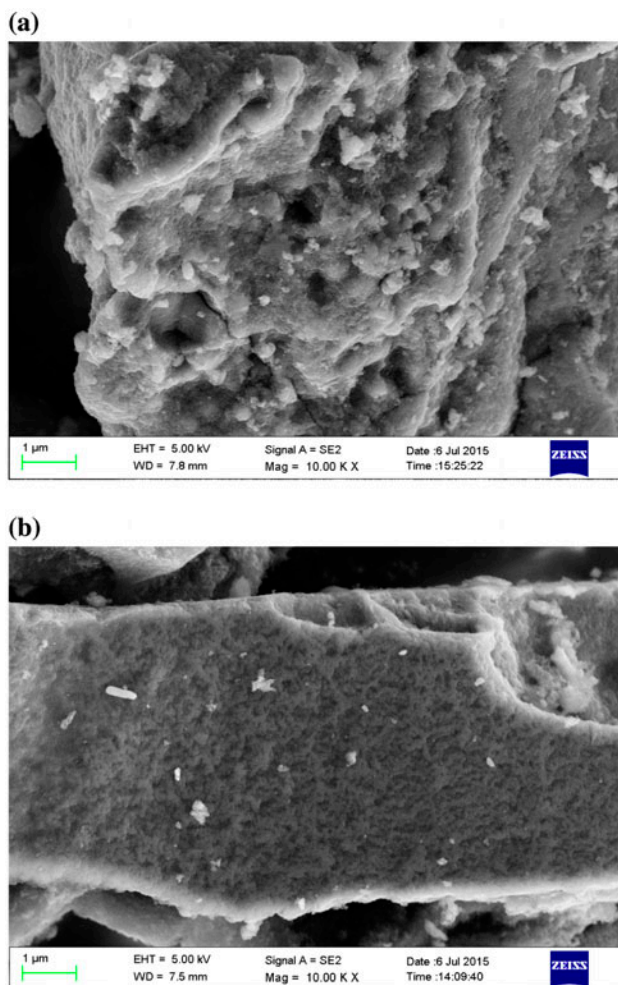
Fig. 1. SEM images of AC-Fe before (a) and after (b) Cr(VI) adsorption.

greatly improved the adsorption performance. Additionally, the oxidation before carbonization had a considerable effect on the textural properties of carbon materials, and the prepared samples were also characterized for their efficiency for Cr(VI) adsorption [26].

To analyze the functional groups of AC-Fe, FTIR spectra of AC-Fe before and after Cr(VI) adsorption were recorded (Fig. 3).The peak at 3,430 cm^{-1} of AC-Fe gets slightly compared with the AC-Fe. The content of O–H or N–H functional groups of AC-Fe is larger than AC. These groups may increase the adsorption property of Cr(VI) [24]. The peak at 1,575.70 cm^{-1} of AC-Fe become gently contrast with the AC-Fe, and the bands in the range 1,500–1,845 cm^{-1} can be ascribed to the presence of aromatic rings, alkenes, ketones, aldehydes, carboxylic acids, and esters groups in hemicellulose compounds or the bond between hemicellulose and lignin [27]. Those functional groups of AC-Fe may dramatically increase and contribute to the adsorption of Cr(VI). The bands at 950–1,300 cm^{-1} indicate the presence of C–O stretching and O–H bending. The bands in the range 400–1,000 cm^{-1} are associated with metal-oxygen and metal-hydroxyl vibrations [28]. Therefore, the adsorption peak at 489.37 cm^{-1} could be attributed to metal-oxygen and metal-hydroxyl bond.

3.2. Effect of contact time

The equilibrium time is an important parameter for uptake of Cr(VI) from aqueous solution, and it is used to predict the feasibility and efficiency of an adsorbent for water treatment [3]. The removal percentages of Cr(VI) from solutions with initial (Cr(VI)) = 10, 20, and 50 mg/L as a function of time are shown
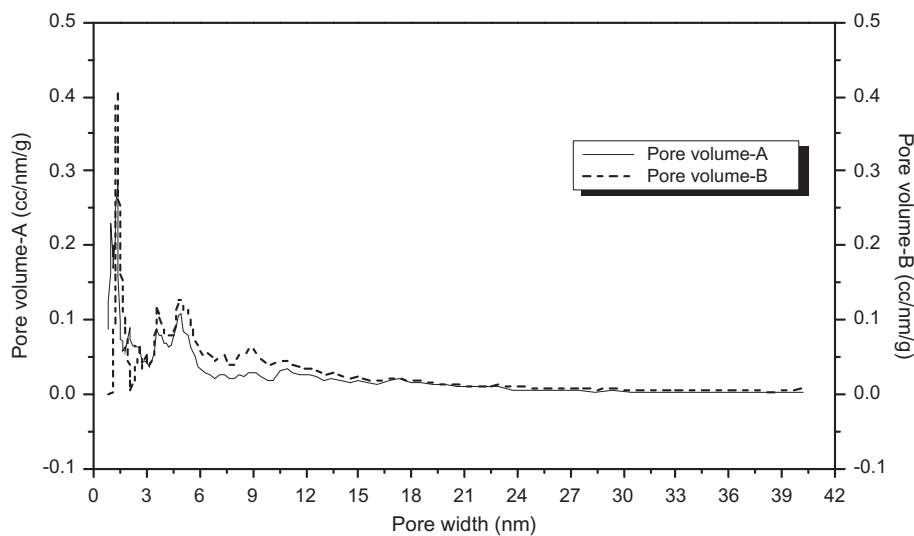
Fig. 2. Pore size distribution of AC (A) and AC-Fe (B) prepared from loofah sponge.
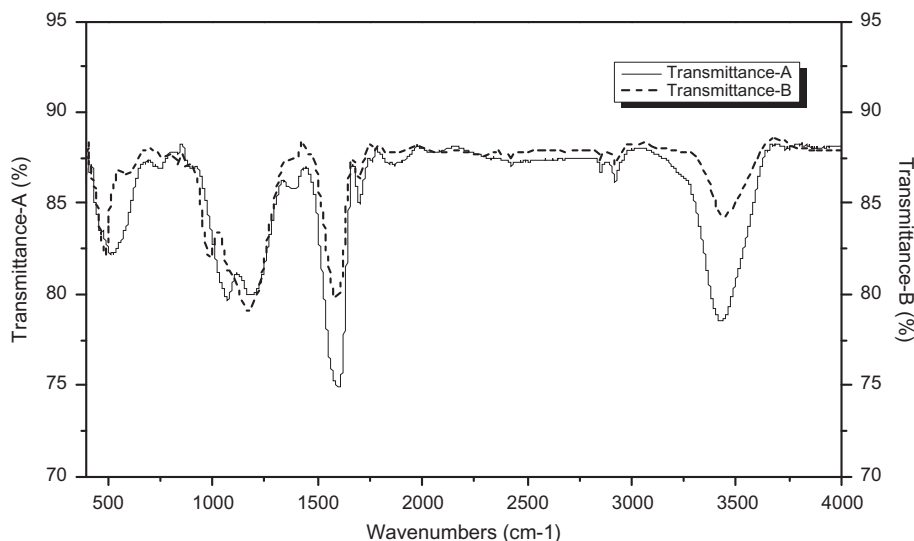
Fig. 3. FTIR spectra of AC-Fe before and after Cr(VI) adsorption.

in Fig. 4. During the first 30 min, the removal rate is very fast. The removal percentage gradually increases from 30 to 240 min and then starts to level off. The removal percentage is lower for higher initial (Cr(VI)) in each time period.

In the initial stages of the adsorption process, the rate Cr(VI) adsorption is fast because there are a large number of available AC-Fe surface adsorption sites. Because of the slow diffusion of solute ions into the bulk of the adsorbent, the rate of adsorption decreases in the later stages of Cr(VI) adsorption [29].

3.3. Effect of temperature

Q_e and the removal efficiency of Cr(VI) are affected by temperature, as shown in Fig. 5. Q_e and the removal efficiency increase with increasing temperature. At 308 K, Q_e = 33.17 mg/g and the removal efficiency is 65.98%, which are about 1.7 times higher than at 288 K. Cr(VI) biosorption is endothermic, so the adsorbed amount increases with increasing temperature [25]. The magnitude of the heat of adsorption can provide useful information about the adsorbed phase and the nature of the surface [30].

3.4. Effect of initial solution pH

The pH greatly influences biosorption of heavy metals [31]. The effect of the initial solution pH on the removal of Cr(VI) by AC-Fe was investigated in the pH range 1–13 with (AC-Fe) = 0.4 g/L and initial (Cr(VI)) = 20 mg/L. The removal efficiency and adsorption capacity of Cr(VI) on AC-Fe as a function of pH are shown in Fig. 6. Q_e rapidly increases with decreasing

pH in the acidic region and decreases with increasing pH in the alkaline region. Maximum adsorption (48.22 mg/L) occurs at pH 1. With increasing pH, the removal efficiency decreases from 98.71% (pH 1) to 3.06% (pH 13). Therefore, acidic conditions improve adsorption of Cr(VI) on AC-Fe.

Various mechanisms can be used to understand the mechanism of Cr(VI) adsorption, such as ion exchange, surface adsorption, complexation, and chemisorption, and two or three mechanisms are usually involved in adsorption of Cr(VI) to the surface of adsorbents [32,33]. $HCrO_4^-$, $Cr_2O_7^{2-}$, and CrO_4^{2-} are the common oxyanions of Cr(VI). $HCrO_4^-$ is dominant in acidic medium, and with increasing pH, it is converted to CrO_4^{2-}. $HCrO_4^-$ is more favorable for sorption than the other species because it has a low adsorption free energy [22].

3.5. Effect of AC-Fe content

The AC-Fe content is an important factor for effective Cr(VI) removal because it determines the sorbent–sorbate equilibrium of the system [34,35]. Fig. 7 shows the effect of AC-Fe content on Q_e and Cr(VI) removal efficiency. From Fig. 7, with increasing AC-Fe content from 0.1 to 0.9 g/L, the removal efficiency of Cr(VI) almost linearly increases from 11.54 to 88.78% and then starts to level off. The maximum removal efficiency is 93.65% at 0.9 g/L. The adsorption capacity is affected by the AC-Fe content. As the AC-Fe content increases, the adsorption capacity first increases and then decreases. The maximum adsorption capacity is 28.75 mg/g at 0.3 g/L.
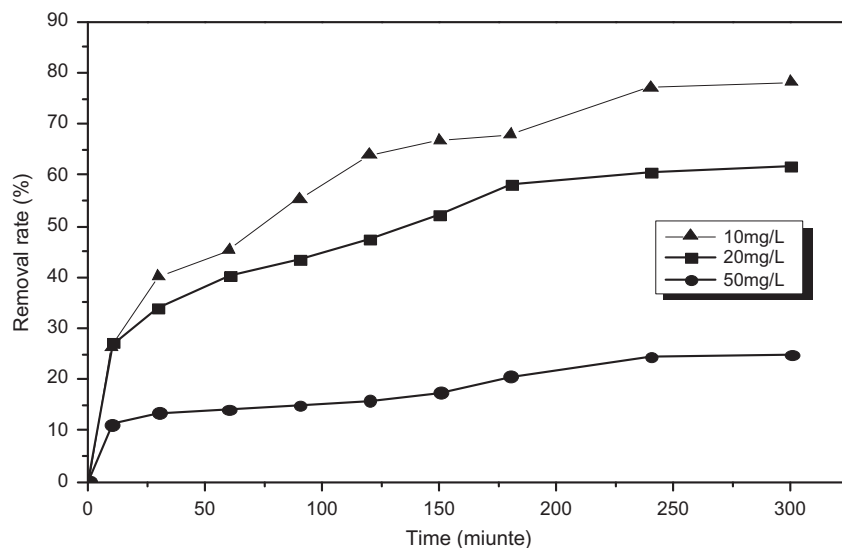
Fig. 4. Effect of contact time on removal rate and adsorption amount (Q_e).
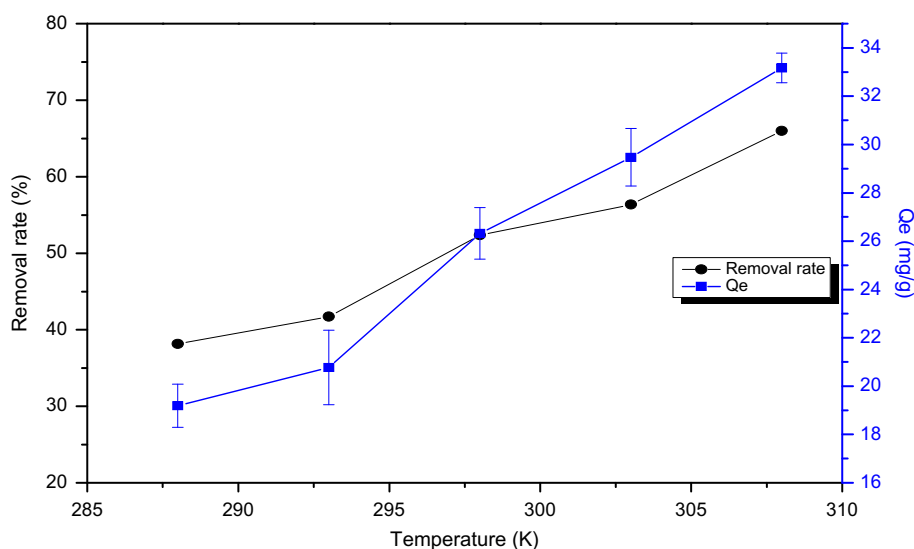
Fig. 5. Effect of temperature on Cr(VI) removal efficiency and adsorption amount (Q_e).

3.6. Effect of initial (Cr(VI))

To overcome the mass transfer resistance of the adsorbate between the aqueous phase and the solid phase in the adsorption process, the driving force is provided by the initial metal ion concentration of the aqueous solution [36].

Fig. 8 shows the effect of the initial (Cr(VI)) on the Cr(VI) removal efficiency and Q_e. As shown in Fig. 8, Q_e increases with increasing initial (Cr(VI)), while the removal efficiency decreases. Q_e rapidly increases while the removal efficiency initially increases and

then decreases with increasing Cr(VI) concentration. At high Cr(VI) concentrations, Q_e slowly increases and the removal efficiency gradually decreases. The maximum removal efficiency is 95.44% at 5 mg/L, and the maximum adsorption amount of Cr(VI) is 34.5 mg/g at 40 mg/L.

3.7. Adsorption isotherm

The adsorption isotherm was investigated for solutions with initial (Cr(VI)) = 1–40 mg/L at
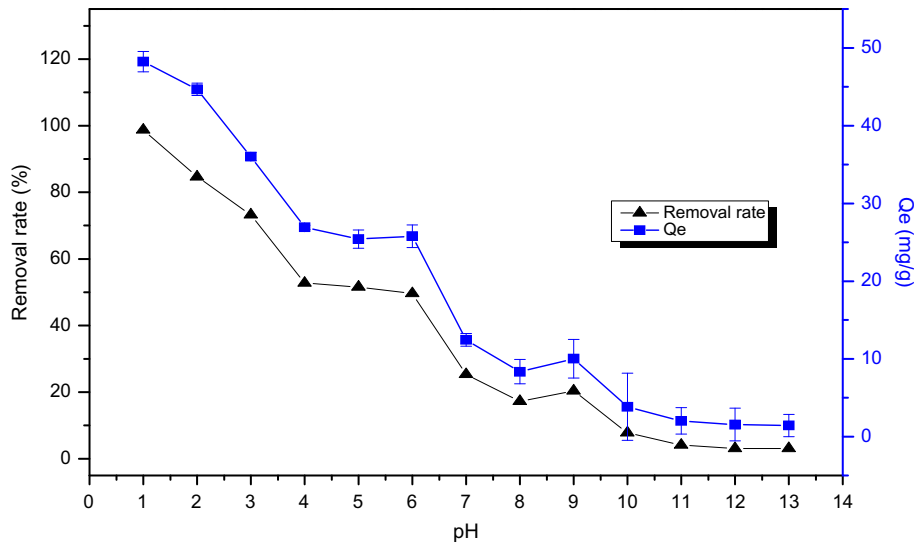
Fig. 6. Effect of solution pH on Cr(VI) removal efficiency and adsorption amount (Q_e) of Cr(VI) on AC-Fe.
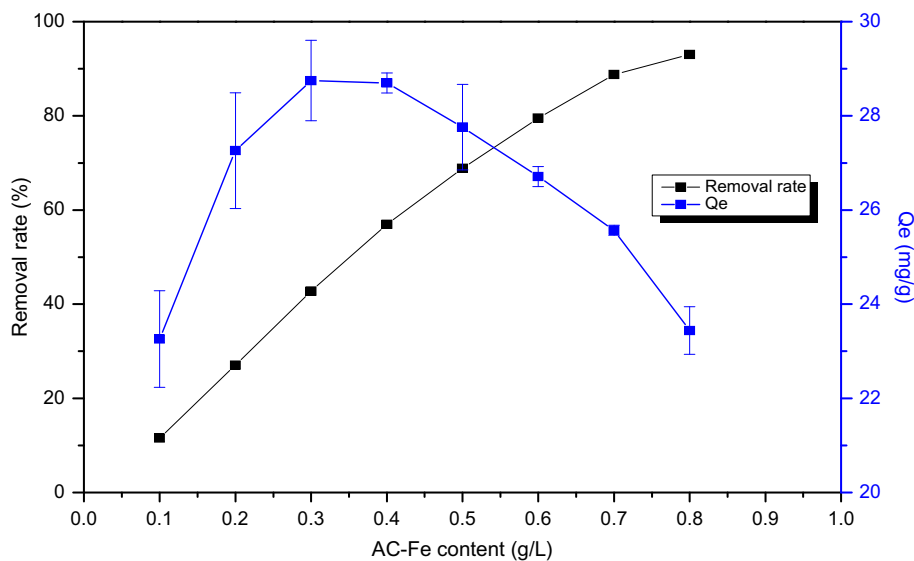
Fig. 7. Effect of AC-Fe content on Cr(VI) removal efficiency and adsorption amount (Q_e).

(AC-Fe) = 0.4 g/L. The maximum Cr(VI) adsorption capacity of AC-Fe was 42 mg/g with the R^2 (=0.9960) at 308 K, observed from the Table 1. In addition, AC-Fe compared with other adsorbent capacity of Cr(VI) is shown in Table 2, which revealed that the AC-Fe has a good adsorption capacity of Cr(VI) [23,37–40]. The Langmuir adsorption isotherm has the highest R^2 value (>0.989), and Q_m is closest to the experimental adsorption amount Q_{exp}. Therefore, the experimental data are best fitted by the Langmuir adsorption isotherm, which assumes monolayer sorption on a surface with a finite number of identical sites [41]. According to isothermal experimental test, the prepared adsorbent indicated relatively fast equilibrium time with monolayer sorption behavior [42].
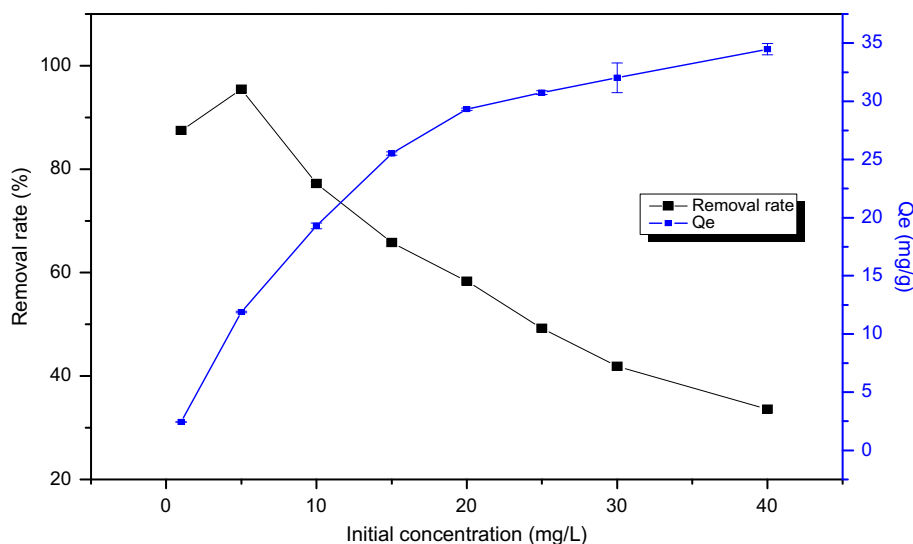
Fig. 8. Effect of the initial (Cr(VI)) on Cr(VI) adsorption amount (Q_e) and removal efficiency.

Table 1
Adsorption isotherms parameters of Cr(VI) on AC-Fe

Adsorption temperature (K)	Q_{exp} (mg/g)	Langmuir			Freundlich			Dubinin–Radushkevich			
		Q_m (mg/g)	K_L (L/mg)	R^2	$1/n$	K_F (mg/g)$^{1/n}$	R^2	Q_m (mg/g)	E (kJ/mol)	β (kJ^2/mol^2)	R^2
288	29.187	29.674	0.599	0.9893	0.381	9.693	0.9369	21.813	22.361	0.001	0.8720
298	34.474	35.842	0.584	0.9959	0.403	11.292	0.8028	29.946	9.129	0.006	0.9607
308	41.950	43.478	0.833	0.9960	0.409	15.097	0.7607	36.387	11.180	0.004	0.9785

Table 2
Comparison of adsorption capacities of Cr(VI) with other adsorbents

Adsorbents	Adsorption capacity (mg/g)	pH	C_0	Refs.
Coconut tree sawdust carbon	3.46	3	20	[23]
HSAC	17.7	2	30	[37]
Sugar cane bagasse	13.4	2	500	[38]
Coconut shell carbon	10.88	4	25	[39]
RAC	44.05	2	200	[40]
Fe-AC	34	1	40	Present study

3.8. Adsorption kinetics

Table 3 shows that the R^2 values are 0.9916, 0.9914, and 0.9835 for the pseudo-second-order model at 288, 298, and 308 K, respectively. Compared with the other two models, the pseudo-second-order model is the most appropriate and Q_e is much closer to Q_{exp}. Based on the assumption that the rate-limiting step for the interaction between the sorbent and sorbate is chemical sorption involving valence forces through the sharing or exchange of electrons [43], the adsorption of Cr(VI) on AC-Fe is a pseudo-second-order reaction. The results

agree with the results of the kinetics of sorption of Cr(VI) to peat (leaf mold) by Sharma and Forster [44,45].

3.9. Thermodynamics

As shown in Table 4, ΔG, ΔS, and ΔH are −1.238 kJ/mol, 84.271 J/(mol K), and 1.204 kJ/mol at 288 K, respectively. The Gibbs free energy indicates the degree of spontaneity of the adsorption process, where a more negative value indicates a more energetically favorable adsorption process. The ΔG values obtained in this study confirm the feasibility of the

Table 3
Kinetic parameters of the pseudo-first-order, pseudo-second-order, and intraparticle diffusion of Cr(VI) on AC-Fe

Adsorption temperature (K)	Q_{exp} (mg/g)	The pseudo-first-order model			The pseudo-second-order model				The intraparticle diffusion model		
		k_1 (min^{-1})	Q_e (mg/g)	R^2	k_2 (g/(mg min))	Q_e (mg/g)	V_0 (mg/(g min))	R^2	k_p (mg/(g min)$^{1/2}$)	C (mg/g)	R^2
288	20.908	0.007	10.349	0.9519	0.0016	21.692	0.750	0.9916	0.641	8.990	0.9557
298	31.038	0.011	22.579	0.9587	0.0008	33.445	0.948	0.9914	1.126	10.991	0.9860
308	34.039	0.013	31.437	0.9346	0.0005	38.168	0.784	0.9835	1.447	8.4774	0.9797

Table 4
Thermodynamic parameters of Cr(VI) on AC-Fe

Temperature (K)	K (L/mol)	ΔG (kJ/mol)	ΔS (J/(mol K))	ΔH (kJ/mol)
288	176.096	−1.238	84.271	1.204
298	171.713	−1.275		
308	245.158	−1.409		

adsorbent and the spontaneity of the adsorption process [41]. The negative ΔG values at all temperatures indicate that the adsorption process is spontaneous in nature. The positive ΔH value indicates the endothermic nature of the adsorption process [46]. The positive ΔS value confirms that there is an increase in randomness at the solid/solution interface for the adsorption of Cr(VI) on AC-Fe [36].

4. Conclusion

The modification method greatly improves the adsorption property. The surface area of the AC was relatively high (834.006 m^2), and the Fe-AC structure was found to be a well-developed array of microvoids and mesopores. FTIR revealed that there was abundance of O–H, N–H, C–O, metal-oxygen, and metal-hydroxyl functional groups on the surface of the Fe-AC, which may increase the adsorption of Cr(VI). Temperature, pH, AC-Fe content, and initial Cr(VI) affect the adsorption process. The equilibrium data agreed well with Langmuir isotherm equation ($R^2 = 0.9960$) at 308 K, which indicated monolayer adsorption, while the limited inner diffusion of Fe-AC structures may greatly reduce the adsorption of Cr(VI) [47]. The adsorption kinetics could be described by the pseudo-second-order model, which was considered as the rate-limiting factor. Thermodynamic analysis confirmed the spontaneity, endothermic nature, and irreversibility of the adsorption process.

Acknowledgements

References

[1] D. Sharma, C. Forster, Column studies into the adsorption of chromium (VI) using sphagnum moss peat, Bioresour. Technol. 52 (1995) 261–267.
[2] I. Singh, D. Singh, Cr(VI) removal in acidic aqueous solution using iron-bearing industrial solid wastes and their stabilisation with cement, Environ. Technol. 23 (2002) 85–95.
[3] S. Chen, Q. Yue, B. Gao, X. Xu, Equilibrium and kinetic adsorption study of the adsorptive removal of Cr(VI) using modified wheat residue, J. Colloid Interface Sci. 349 (2010) 256–264.
[4] G. Bayramoglu, M.Y. Arica, Adsorption of Cr(VI) onto PEI immobilized acrylate-based magnetic beads: Isotherms, kinetics and thermodynamics study, Chem. Eng. J. 139 (2008) 20–28.
[5] H. Song, Y. Liu, W. Xu, G. Zeng, N. Aibibu, L. Xu, B. Chen, Simultaneous Cr(VI) reduction and phenol degradation in pure cultures of *Pseudomonas aeruginosa* CCTCC AB91095, Bioresour. Technol. 100 (2009) 5079–5084.
[6] L. Lin, X. Xu, C. Papelis, T.Y. Cath, P. Xu, Sorption of metals and metalloids from reverse osmosis concentrate on drinking water treatment solids, Sep. Purif. Technol. 134 (2014) 37–45.
[7] S.A. Cavaco, S. Fernandes, M.M. Quina, L.M. Ferreira, Removal of chromium from electroplating industry effluents by ion exchange resins, J. Hazard. Mater. 144 (2007) 634–638.

[8] V.K. Gupta, R. Jain, A. Mittal, T.A. Saleh, A. Nayak, S. Agarwal, S. Sikarwar, Photo-catalytic degradation of toxic dye amaranth on TiO_2/UV in aqueous suspensions, Mater. Sci. Eng. C 32 (2012) 12–17.

[9] T.A. Saleh, V.K. Gupta, Photo-catalyzed degradation of hazardous dye methyl orange by use of a composite catalyst consisting of multi-walled carbon nanotubes and titanium dioxide, J. Colloid Interface Sci. 371 (2012) 101–106.

[10] R.R. Dash, C. Balomajumder, A. Kumar, Treatment of metal cyanide bearing wastewater by simultaneous adsorption and biodegradation (SAB), J. Hazard. Mater. 152 (2008) 387–396.

[11] M.A. Salam, R.M. El-Shishtawy, A.Y. Obaid, Synthesis of magnetic multi-walled carbon nanotubes/magnetite/chitin magnetic nanocomposite for the removal of Rose Bengal from real and model solution, J. Ind. Eng. Chem. 20 (2014) 3559–3567.

[12] T.A. Saleh, V.K. Gupta, Column with CNT/magnesium oxide composite for lead (II) removal from water, Environ. Sci. Pollut. Res. 19 (2012) 1224–1228.

[13] T.A. Saleh, V.K. Gupta, Processing methods, characteristics and adsorption behavior of tire derived carbons: A review, Adv. Colloid Interface Sci. 211 (2014) 93–101.

[14] V. Gupta, S. Agarwal, T.A. Saleh, Chromium removal by combining the magnetic properties of iron oxide with adsorption properties of carbon nanotubes, Water Res. 45 (2011) 2207–2212.

[15] Y. Guo, J. Qi, S. Yang, K. Yu, Z. Wang, H. Xu, Adsorption of Cr(VI) on micro-and mesoporous rice husk-based active carbon, Mater. Chem. Phys. 78 (2003) 132–137.

[16] M. Owlad, M.K. Aroua, W.M.A.W. Daud, Hexavalent chromium adsorption on impregnated palm shell activated carbon with polyethyleneimine, Bioresour. Technol. 101 (2010) 5098–5103.

[17] W. Liu, J. Zhang, C. Zhang, Y. Wang, Y. Li, Adsorptive removal of Cr(VI) by Fe-modified activated carbon prepared from *Trapa natans* husk, Chem. Eng. J. 162 (2010) 677–684.

[18] K. Periasamy, K. Srinivasan, P. Murugan, Studies on chromium (VI) removal by activated groundnut husk carbon, Indian J. Environ. Health 33 (1991) 433–439.

[19] M.-s. Miao, Y.-n. Wang, Q. Kong, L. Shu, Adsorption kinetics and optimum conditions for Cr(VI) removal by activated carbon prepared from luffa sponge, Desalin. Water Treat. 57 (2016) 7763–7772.

[20] X. Xu, B.-Y. Gao, X. Tang, Q.-Y. Yue, Q.-Q. Zhong, Q. Li, Characteristics of cellulosic amine-crosslinked copolymer and its sorption properties for Cr(VI) from aqueous solutions, J. Hazard. Mater. 189 (2011) 420–426.

[21] A. Gupta, C. Balomajumder, Simultaneous adsorption of Cr(VI) and phenol onto tea waste biomass from binary mixture: Multicomponent adsorption, thermodynamic and kinetic study, J. Environ. Chem. Eng. 3 (2015) 785–796.

[22] P. Yuan, M. Fan, D. Yang, H. He, D. Liu, A. Yuan, J. Zhu, T. Chen, Montmorillonite-supported magnetite nanoparticles for the removal of hexavalent chromium [Cr(VI)] from aqueous solutions, J. Hazard. Mater. 166 (2009) 821–829.

[23] K. Selvi, S. Pattabhi, K. Kadirvelu, Removal of Cr(VI) from aqueous solution by adsorption onto activated carbon, Bioresour. Technol. 80 (2001) 87–89.

[24] T. Tay, S. Ucar, S. Karagöz, Preparation and characterization of activated carbon from waste biomass, J. Hazard. Mater. 165 (2009) 481–485.

[25] S.I. Lyubchik, A.I. Lyubchik, O.L. Galushko, L.P. Tikhonova, J. Vital, I.M. Fonseca, S.B. Lyubchik, Kinetics and thermodynamics of the Cr(III) adsorption on the activated carbon from co-mingled wastes, Colloids Surf. A: Physicochem. Eng. Aspects 242 (2004) 151–158.

[26] Z.A. AL-Othman, R. Ali, M. Naushad, Hexavalent chromium removal from aqueous medium by activated carbon prepared from peanut shell: Adsorption kinetics, equilibrium and thermodynamic studies, Chem. Eng. J. 184 (2012) 238–247.

[27] A. Kumar, H.M. Jena, High surface area microporous activated carbons prepared from Fox nut (Euryale ferox) shell by zinc chloride activation, Appl. Surf. Sci. 356 (2015) 753–761.

[28] Z. Ai, Y. Cheng, L. Zhang, J. Qiu, Efficient removal of Cr(VI) from aqueous solution with Fe@ Fe_2O_3 core−shell nanowires, Environ. Sci. Technol. 42 (2008) 6955–6960.

[29] S. Gupta, B. Babu, Removal of toxic metal Cr(VI) from aqueous solutions using sawdust as adsorbent: Equilibrium, kinetics and regeneration studies, Chem. Eng. J. 150 (2009) 352–365.

[30] Y.A. El-Reash, M. Otto, I. Kenawy, A. Ouf, Adsorption of Cr(VI) and As(V) ions by modified magnetic chitosan chelating resin, Int. J. Biol. Macromol. 49 (2011) 513–522.

[31] V. Venugopal, K. Mohanty, Biosorptive uptake of Cr (VI) from aqueous solutions by *Parthenium hysterophorus* weed: Equilibrium, kinetics and thermodynamic studies, Chem. Eng. J. 174 (2011) 151–158.

[32] R.H. Crist, J.R. Martin, J. Chonko, D.R. Crist, Uptake of metals on peat moss: An ion-exchange process, Environ. Sci. Technol. 30 (1996) 2456–2461.

[33] S. Baral, N. Das, G.R. Chaudhury, S. Das, A preliminary study on the adsorptive removal of Cr(VI) using seaweed, Hydrilla verticillata, J. Hazard. Mater. 171 (2009) 358–369.

[34] M.A. Hanif, R. Nadeem, H.N. Bhatti, N.R. Ahmad, T.M. Ansari, Ni(II) biosorption by *Cassia fistula* (golden shower) biomass, J. Hazard. Mater. 139 (2007) 345–355.

[35] N. Ahalya, R. Kanamadi, T. Ramachandra, Biosorption of chromium(VI) from aqueous solutions by the husk of Bengal gram (*Cicer arientinum*), Electron. J. Biotechnol. 8 (2005) 258–264.

[36] S. Yadav, V. Srivastava, S. Banerjee, C.-H. Weng, Y.C. Sharma, Adsorption characteristics of modified sand for the removal of hexavalent chromium ions from aqueous solutions: Kinetic, thermodynamic and equilibrium studies, Catena 100 (2013) 120–127.

[37] G. Cimino, A. Passerini, G. Toscano, Removal of toxic cations and Cr(VI) from aqueous solution by hazelnut shell, Water Res. 34 (2000) 2955–2962.

[38] D. Sharma, C. Forster, A preliminary examination into the adsorption of hexavalent chromium using low-cost adsorbents, Bioresour. Technol. 47 (1994) 257–264.

[39] S. Babel, T.A. Kurniawan, Cr(VI) removal from synthetic wastewater using coconut shell charcoal and commercial activated carbon modified with oxidizing agents and/or chitosan, Chemosphere 54 (2004) 951–967.

[40] E. Demirbas, M. Kobya, E. Senturk, T. Ozkan, Adsorption kinetics for the removal of chromium(VI) from aqueous solutions on the activated carbons prepared from agricultural wastes, Water S. A. 30 (2004) 533–540.

[41] A. Bhattacharya, T. Naiya, S. Mandal, S. Das, Adsorption, kinetics and equilibrium studies on removal of Cr(VI) from aqueous solutions using different low-cost adsorbents, Chem. Eng. J. 137 (2008) 529–541.

[42] A. Shahat, M.R. Awual, M.A. Khaleque, M.Z. Alam, M. Naushad, A.S. Chowdhury, Large-pore diameter nano-adsorbent and its application for rapid lead(II) detection and removal from aqueous media, Chem. Eng. J. 273 (2015) 286–295.

[43] Y.-S. Ho, G. McKay, Pseudo-second order model for sorption processes, Process Biochem. 34 (1999) 451–465.

[44] D. Sharma, C. Forster, Removal of hexavalent chromium using sphagnum moss peat, Water Res. 27 (1993) 1201–1208.

[45] D. Sharma, C. Forster, The treatment of chromium wastewaters using the sorptive potential of leaf mould, Bioresour. Technol. 49 (1994) 31–40.

[46] Q. Kong, Y.-n. Wang, L. Shu, M.-s. Miao, Isotherm, kinetic, and thermodynamic equations for cefalexin removal from liquids using activated carbon synthesized from loofah sponge, Desalin. Water Treat. 57 (2016) 7733–7742.

[47] Z. Li, T. Li, L. An, H. Liu, L. Gu, Z. Zhang, Preparation of chitosan/polycaprolactam nanofibrous filter paper and its greatly enhanced chromium (VI) adsorption, Colloids Surf. A Physicochem. Eng. Aspects 494 (2016) 65–73.